

## A STATE CHANGE IN THE MISSING LINK BINARY PULSAR SYSTEM PSR J1023+0038

B. W. STAPPERS<sup>1</sup>, A. M. ARCHIBALD<sup>2</sup>, J. W. T. HESSELS<sup>2,3</sup>, C. G. BASSA<sup>2</sup>, S. BOGDANOV<sup>4</sup>, G. H. JANSSEN<sup>2</sup>, V. M. KASPI<sup>5</sup>, A. G. LYNE<sup>1</sup>, A. PATRUNO<sup>6,2</sup>, S. TENDULKAR<sup>7</sup>, A. B. HILL<sup>8,9</sup>, T. GLANZMAN<sup>8</sup>

*Draft version December 2, 2013*

### Abstract

We present radio, X-ray, and  $\gamma$ -ray observations which reveal that the binary millisecond pulsar / low-mass X-ray binary transition system PSR J1023+0038 has undergone a transformation in state. Whereas until recently the system harbored a bright millisecond radio pulsar, the radio pulsations at frequencies between 300 to 5000 MHz have now become undetectable. Concurrent with this radio disappearance, the  $\gamma$ -ray flux of the system has quintupled. We conclude that, though the radio pulsar is currently not detectable, the pulsar mechanism is still active and the pulsar wind, as well as a newly formed accretion disk, are together providing the necessary conditions to create the  $\gamma$ -ray increase. The system is the first example of a transient, compact, low-mass  $\gamma$ -ray binary and will continue to provide an exceptional test bed for better understanding the formation of millisecond pulsars as well as accretion onto neutron stars in general.

*Subject headings:* X-rays: binaries — gamma-rays: binaries — pulsars: individual (PSR J1023+0038)

### 1. INTRODUCTION

The pulsar “recycling” scenario (Alpar et al. 1982; Radhakrishnan & Srinivasan 1981) proposes that the rapid rotation rates of millisecond pulsars (MSPs<sup>10</sup>) originate from a period of mass accretion from a binary companion in a low-mass X-ray binary (LMXB). The idea that such systems could also result in the complete ablation of the companion star and produce isolated MSPs — like the first MSP discovered, PSR B1937+21 (Backer et al. 1982) — seemed to be confirmed by the discovery of the first eclipsing “black widow” pulsar PSR B1957+20 (Fruchter et al. 1990). The eclipses of the radio pulsations in this system showed that mass was being ablated from the very low mass ( $M_c \ll 0.1 M_\odot$ ) companion (Ryba & Taylor 1991), however the mass loss rate appeared to be insufficient to ever completely destroy the

companion. The LMXB and ablation phases were expected to be short-lived and so the subsequent discovery of another black widow, PSR J2051–0827 (Stappers et al. 1996), seemed to challenge the connection between these systems and the isolated MSPs. Nonetheless, clear evidence that MSPs are indeed spun-up in LMXBs came with the discovery of coherent X-ray pulsations at a period of 2.5 ms from the LMXB SAX J1808.4–3658 during an X-ray outburst (Wijnands & van der Klis 1998). To date there are some 15 of these accreting X-ray millisecond pulsars (AMXPs) known (Patruno & Watts 2012).

With the rapid rate of MSP discoveries in the last few years (Ransom 2013, see his Fig. 1), the diversity of MSP binary companions has continued to grow beyond the standard low-mass white dwarf or ultra-low-mass black widow companions that were initially found. This variety has shown that the pulsar recycling process produces a rich array of systems, some of which are exceedingly exotic (e.g., Bailes et al. 2011). Furthermore, some of these new systems are excellent case studies for better understanding the accretion-induced spin-up of neutron stars.

Recently, a completely new class of eclipsing binary MSP systems, dubbed “redbacks”, with more massive ( $M_c \gtrsim 0.1 M_\odot$ ) and likely non-degenerate companions have been discovered (Roberts 2011 and references therein). Targeted searches for radio pulsars in unassociated *Fermi*  $\gamma$ -ray sources have been particularly fruitful, producing the majority of these discoveries (Ray et al. 2012; Hessels et al. 2011). Such searches have also found many more examples of the previously known black widow systems. It has also been shown that during the accretion stage the companion star can be ablated down to the mass of a planet (Bailes et al. 2011; van Haaften et al. 2012) while at the same time (barely) surviving complete destruction via ablation. This again suggests that in some cases the companion does not survive and an isolated MSP is left behind.

With the wide variety of MSP systems now known, it is necessary to better understand the various poten-

<sup>1</sup> Jodrell Bank Centre for Astrophysics, School of Physics and Astronomy, The University of Manchester, Manchester M13 9PL, UK

<sup>2</sup> ASTRON, the Netherlands Institute for Radio Astronomy, Postbus 2, 7990 AA Dwingeloo, the Netherlands

<sup>3</sup> Astronomical Institute A.Pannekoek, University of Amsterdam, 1098XH, Amsterdam, the Netherlands

<sup>4</sup> Columbia Astrophysics Laboratory, Columbia University, 550 West 120th Street, New York, NY 10027, USA

<sup>5</sup> McGill University, 3600 University Street, Montreal, QC H3A 2T8, Canada

<sup>6</sup> Leiden Observatory, Leiden University, PO Box 9513, NL-2300 RA Leiden, the Netherlands

<sup>7</sup> Space Radiation Laboratory, California Institute of Technology, 1200 E California Blvd, MC 249-17, Pasadena, CA 91125, USA

<sup>8</sup> W. W. Hansen Experimental Physics Laboratory, KIPAC, Department of Physics and SLAC National Accelerator Laboratory, Stanford University, Stanford, CA 94305, USA

<sup>9</sup> Faculty of Physical & Applied Sciences, University of Southampton, Highfield, Southampton, SO17 1BJ, UK

<sup>10</sup> We use the term MSP for a neutron star rotating with a period  $P_{\text{spin}} \lesssim 30$  ms and with an inferred surface magnetic field  $B_{\text{surf}} \lesssim 10^{10}$  G. Such sources derive their power from the star’s rotational kinetic energy loss and necessarily produce observable radio pulsations. In an increasing number of cases pulsed magnetospheric emission is also detected in keV X-rays and MeV–GeV  $\gamma$ -rays.

tial accretion and ablation processes in LMXBs and eclipsing binary MSPs. While most MSP systems are clearly well past any accretion episode, the redbacks and black widows appear to provide the closest available link to the LMXBs. There are now two exceptional systems, the Galactic field binary pulsar J1023+0038 (hereafter J1023; Archibald et al. 2009) and PSR J1824–2452I/IGR J18245–2452 (hereafter M28I; Papitto et al. 2013), located in the globular cluster (GC) M28. Both are providing us with a detailed look at the transition between these two phases. In fact, the behavior of these two systems in the last decade has made it abundantly clear that the transition between an LMXB and an MSP is not a sudden or unidirectional transformation.

J1023 was discovered in 2007 as a 1.7-ms radio pulsar in a 4.8-hour circular-orbit eclipsing binary system. It was soon recognized to be the same source as FIRST J102347.6+003841, which had originally been identified as a magnetic cataclysmic variable (Bond et al. 2002) but was subsequently shown to have been an LMXB with an accretion disk during 2001 (Thorstensen & Armstrong 2005). Later optical and X-ray observations indicated that the source no longer possessed an accretion disk (Woudt et al. 2004; Homer et al. 2006; Archibald et al. 2009, 2010; Bogdanov et al. 2011). It was therefore identified as the first object to have been seen to transition from an LMXB to an MSP. Archibald et al. (2013) also show that since its discovery as a pulsar this “original redback” has exhibited radio behavior typical of this class of eclipsing binary MSPs. During this phase, X-rays are produced by the system (Archibald et al. 2010; Bogdanov et al. 2011) but they originate from a combination of pulsed magnetospheric emission and an intra-binary shock between the companion and MSP winds.

M28I links LMXBs and MSPs in a complementary way because it has been seen to transition from a radio emitting MSP to an AMXP: i.e. it has shown accretion-powered pulsations at the same rotational period as the previously known radio pulsar (Papitto et al. 2013). Moreover, it was suggested that this object has been seen to swing between these states several times over the past decade.

Here we report a sudden change of state in J1023, starting in 2013 June. This change was heralded by the cessation of detectable pulsed radio emission from the MSP and coincides with a dramatic, five-fold increase in the  $\gamma$ -ray flux from the system. Along with the reported changes in the X-ray behavior (Patruno et al. 2013) and the emergence of double-peaked optical spectral lines (Halpern et al. 2013), this points to an accretion disk having re-formed in the system *but* with a still-active pulsar mechanism also present.

## 2. OBSERVATIONS AND DATA REDUCTION

### 2.1. Radio observations

As part of a campaign to track the spin and orbital evolution of the J1023 system, we are regularly observing it with the 76-m Lovell Telescope (LT) at Jodrell Bank in the United Kingdom and the 94-m (equivalent) Westerbork Synthesis Radio Telescope (WSRT) in the Netherlands. We observed using the LT on average

once every 10 days, with a typical duration of 30 min. Since 2013 July, we are observing with 1-hr integrations approximately weekly. The LT observations are centered at 1500 MHz and were recorded using both a digital filter bank (DFB) and, as of 2011 April, a coherent dedispersion system (ROACH) in parallel. The DFB and ROACH both provide 384 MHz of usable bandwidth after interference excision; the primary advantage of the ROACH data is simply that it provides higher effective time resolution after dedispersion using DSPSR (van Straten & Bailes 2011). We used WSRT in tied-array mode (where the signals from all the available dishes are summed in phase) at central frequencies of 350 and 1380 MHz with respective bandwidths of 80 and 160 MHz. For both observing bands the data were coherently dedispersed using the PuMaII backend (Karuppusamy et al. 2008). Typically we observed for 25 min, but since 2013 July a number of longer observations, up to a full orbit, have been made. For both the LT and WSRT, data inspection and post processing, including dedispersion optimization and interference removal, is done using the PSRCHIVE<sup>11</sup> package (van Straten et al. 2012). The archived data products have 10-s time resolution to search for short timescale changes in brightness.

In addition to our regular LT/WSRT monitoring, we have taken two long observations using the Green Bank Telescope (GBT) on 2013 August 11 and the Arecibo telescope (AO) on 2013 August 28, at central frequencies of 2 GHz and 4.5 GHz, respectively. At the GBT, we used the GUPPI pulsar backend to coherently dedisperse an 800-MHz band. The accumulated profiles were written to disk every 2.64 s. With AO, we ran seven Mock spectrometers, each recording 172 MHz, in parallel which spanned the total available 1-GHz band after removing overlap. The band was divided into 256 channels, recorded every 32.768  $\mu$ s. DSPSR was used to incoherently dedisperse the data and fold it into 32 pulse phase bins, writing out a profile every 100 s. The various radio observing systems are summarized in Table 1.

**Table 1**  
Parameters of the radio telescopes used

Telescope	LT	WSRT	WSRT	GBT	AO
Frequency (MHz)	1500	350	1380	2300	4500
Bandwidth (MHz)	384	80	160	800	1000
$T_{\text{sys}}$ (K)	27	150	25	25	25
Gain (K Jy <sup>-1</sup> )	1.0	1.0	1.0	2.0	10.0

### 2.2. Gamma-ray observations

J1023 is spatially associated with a  $\gamma$ -ray source detected while J1023 was active as a radio MSP (2FGL J1023.6+0040; Tam et al. 2010; Nolan et al. 2012; Archibald et al. 2013). In light of this association, and of the possibility of a change due to the disappearance of an observable radio pulsar, we investigated the  $\gamma$ -ray light curve. We retrieved the *Fermi* Large Area Telescope (LAT; Atwood et al. 2009) Pass 7 reprocessed photons with energies of 100 MeV – 300 GeV from the time

<sup>11</sup> <http://psrchive.sourceforge.net/>

range 2008 August 9 to 2013 November 18. We used the *Fermi* science tools version v9r32p5 for our analysis. We selected those photons with the SOURCE event class, and maximum zenith angle  $100^\circ$  to reduce contamination from atmospheric  $\gamma$ -rays. The light curve analysis was then performed using two approaches, which we now describe in turn.

The first approach follows the *Fermi* Cicerone<sup>12</sup> on aperture photometry. We selected the  $>1$  GeV photons, for which the point-spread function radius is  $\lesssim 1^\circ$  (Ackermann et al. 2012), that were within  $1^\circ$  of J1023. For reference, the nearest source in the 2FGL catalog is  $2^\circ$  away. We then applied a region of interest (ROI) cut, filtered by the data selection (DATA\_QUAL==1) && (LAT\_CONFIG==1) && ABS(ROCK\_ANGLE)<52, and computed good time intervals (GTIs). We binned the resulting photons into 500-ks time bins and used the gtexposure tool with the P7REP\_SOURCE\_V15 instrument response functions, assuming a spectral index of 2.5 (the 2FGL catalog gives a spectral index for the associated source of  $2.5 \pm 0.3$ ; Nolan et al. 2012), to compute the effective exposure within each bin. This left us with 260 photons before the disappearance and 63 after. We then re-binned the light curve and exposure values into 2.5-Ms bins and plotted the resulting light curve, assuming Poisson errors.

The second approach follows the *Fermi* Cicerone on binned likelihood fitting. We again applied the same ROI cut, data selection, and GTIs as above to all our photons. We constructed live time cubes, exposure maps, and source maps for a  $40^\circ \times 40^\circ$  square region. We extracted an XML<sup>13</sup> sky model for all sources within a  $35^\circ$  circular region centered on J1023 from the 2FGL sky survey data<sup>14</sup>. This model uses a log-parabola spectral model for J1023 and the public diffuse models g11\_iem\_v05 and iso\_sourcev05.txt. In this sky model we kept the normalization free for all sources within  $6^\circ$  of J1023; all other parameters, including normalizations for sources further away, were held fixed. We used this model to extract light curves for all sources within  $6^\circ$  of J1023. This process involved making a series of 5-Ms sub-selections from our photon list. We applied the above spectral fitting process — generating live time cubes, exposure maps, and source maps, then fitting our amplitude model — to each sub-selection. For those bins in which J1023 had Test Statistic less than 9 we used the python likelihood tools to compute 95% upper limits. Finally we plotted the reported flux and errors or upper limits for J1023 within each sub-selection, along with long-term average fluxes and their errors for the pre-disappearance and post-disappearance spans.

In addition to building a light curve, we compiled a list of photons possibly originating from J1023. To do this, we selected all photons within  $30^\circ$  of J1023 and used the tool gtsrcprob, with the spectral model taken from the 2FGL catalog described above, to assign each photon a probability of having come from J1023. Using simulations we determined that the low-probability photons play no role in modulation testing, so we discarded all photons with a probability less than 0.001. We used

these photons to search for orbital or rotational modulation in the  $\gamma$ -ray flux from J1023.

### 2.3. X-ray observations

To monitor the X-ray behavior of J1023, we used the publicly available data recorded with the *Swift*/BAT Hard X-ray monitor (Krimm et al. 2013) to generate a 15 – 50 keV X-ray light curve from the period 2013 June 1 to November 2, excluding the period from August 23 to September 9, during which Solar constraints prevented observations. The daily *Swift*/BAT sensitivity has an average value of  $2 \times 10^{35}$  erg s<sup>-1</sup>. Variations in the daily exposure times, however, can change the sensitivity between  $9 \times 10^{34}$  erg s<sup>-1</sup> and  $10^{36}$  erg s<sup>-1</sup>. The coded exposure time (i.e., the exposure time rescaled by the fractional coding) varies between  $\sim 100$  and  $\sim 20000$  seconds.

## 3. RESULTS

### 3.1. Radio results

A summary of the radio observations made with the LT and WSRT since 2009 is presented in Figure 1, where circles represent clear detections of pulsed emission and all other symbols indicate non-detections. This plot shows clearly the effect of the eclipses around orbital phase 0.25, when the pulsar is behind its companion. The eclipse duration approaches 50% at low radio frequencies (red symbols); see Archibald et al. (2013) for a detailed discussion. Variability away from eclipse in the L-band (1380 MHz and 1500 MHz) observations (black symbols) is caused by strong scintillation in the interstellar medium, shown to have a bandwidth of about 100 MHz (Archibald et al. 2013) at this frequency, and as expected for a pulsar with a dispersion measure of only 14.3 pc cm<sup>-3</sup>. The 350-MHz observations have a sufficiently large fractional bandwidth that they are unaffected by scintillation, but the eclipses are longer and there are also short duration, up to a few minutes long, eclipses at other orbital phases. Apart from this variability, the most obvious feature in Figure 1 is that there has been no detection of pulsed radio emission from the pulsar since mid June 2013. It may be that J1023 is still an un-pulsed radio source but the observations reported here are unable to determine if that is the case<sup>15</sup>.

Inspection of the regular LT timing observations in mid July revealed that pulsations had not been detected since 2013 May 31 at 1500 MHz. A check of the WSRT 350 MHz and 1380 MHz observations showed that the source was last detected on 2013 June 15. Increasing the cadence and duration of observations quickly revealed that the pulsed radio emission was no longer seen at any of these frequencies. Using the telescope and backend parameters given in Table 1 we derive  $10\sigma$  flux density upper limits of 0.8 and 0.06 mJy for WSRT 350-MHz and LT 1500-MHz observations, respectively. These limits are more than an order of magnitude lower than the typical flux densities of 16 and 0.9 mJy measured between 2009 April and 2013 June. These limits rule out that the sudden disappearance is due to scintillation.

<sup>15</sup> While the WSRT is a synthesis telescope and could in theory make an image of the source, it is an East-West array and the source is located at the celestial equator which, when combined with our relatively short integration times, makes imaging almost impossible.

<sup>12</sup> <http://fermi.gsfc.nasa.gov/ssc/data/analysis/documentation/Cicerone/>

<sup>13</sup> Extensible Markup Language

<sup>14</sup> [http://fermi.gsfc.nasa.gov/ssc/data/access/lat/2yr\\_catalog/](http://fermi.gsfc.nasa.gov/ssc/data/access/lat/2yr_catalog/)

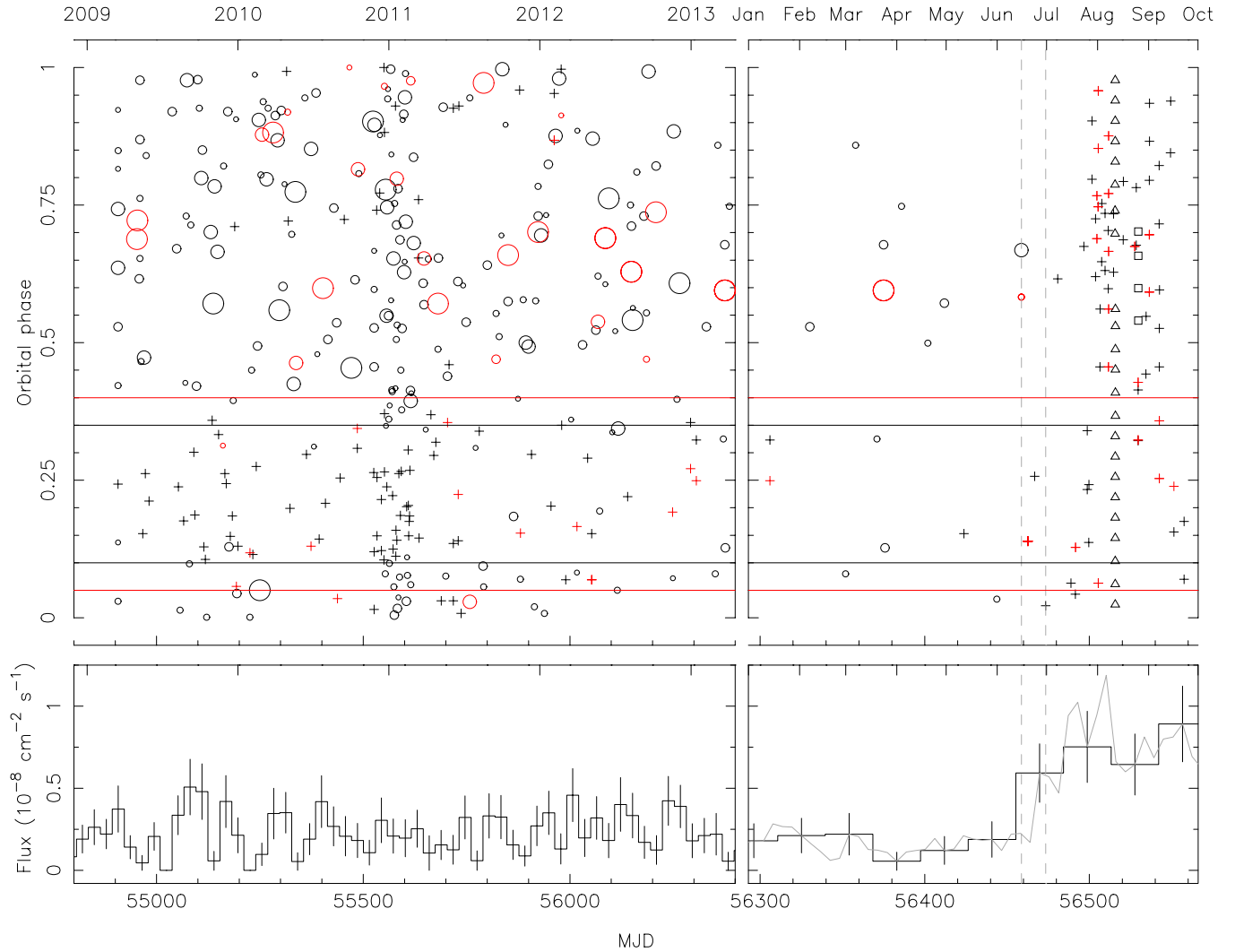


**Figure 1.** Timeline for the state change in J1023. Top panel: Radio observations of J1023 with the LT at 1500 MHz and WSRT at 1380 MHz (black symbols), WSRT at 350 MHz (red symbols), GBT at 2 GHz (triangles) and Arecibo at 4.5 GHz (squares). The observations are plotted against time and orbital phase, where an orbital phase of zero has the pulsar passing the ascending node. The left panel shows data from 2009 to 2013, while the right panel shows the data from 2013. Observations where the pulsar was not detected are denoted by pluses, triangles and squares, while detections are shown by circles, with the circle size indicating the signal-to-noise of the detection. The horizontal lines show the average eclipse duration at 1380 and 1500 MHz (black) and 350 MHz (red). The vertical dashed lines indicate the last confirmed detection on 2013 June 15 of the pulsed signal and the first non-detection outside the known eclipse region on 2013 June 30. Bottom panel: 1–300 GeV  $\gamma$ -ray photon flux computed with aperture photometry. The steps (solid line) show the flux averaged over 2.5-Ms segments, with Poisson errors. The grey line shows the result of taking the same 2.5-Ms averages with intermediate starting points, effectively convolving the photon arrival time series with a 2.5-Ms top-hat function.

As shown in Archibald et al. (2009, 2013), the eclipse durations are strongly frequency dependent (as well as varying somewhat between orbits). This motivated the higher-frequency GBT and AO observations (the triangle and square symbols in Figure 1, respectively). A full orbit was sampled with the GBT observations and the AO observations spanned orbital phases of 0.5–0.75, away from the low-frequency eclipse region. No pulsed radio emission was detected down to  $10\sigma$  flux density limits of 0.016 and 0.003 mJy at 2 GHz and 4.5 GHz, respectively. These non-detections confirm that the J1023 system changed to a different state sometime between 2013 June 15 and 2013 June 30. The lack of observable radio pulsations indicates that either the radio pulsar mechanism has been extinguished or the radio pulsations are undetectable because they are scattered in time or com-

pletely absorbed by an increase of intra-binary material. This state has persisted until at least 2013 November.

### 3.2. Gamma-ray results

Figure 2 shows that the  $\gamma$ -ray flux has increased dramatically since the radio disappearance. This conclusion is consistently reached using both of the analysis methods described in §2. Specifically, the average pre-disappearance  $\gamma$ -ray flux<sup>16</sup> obtained by spectral fitting is  $1.05(11) \times 10^{-8} \text{ cm}^{-2} \text{ s}^{-1}$ , while the average post-disappearance flux is  $6.3(6) \times 10^{-8} \text{ cm}^{-2} \text{ s}^{-1}$ . By comparison, the fluxes obtained from aperture pho-

<sup>16</sup> Number(s) shown in parentheses represent the statistical uncertainty in the last digit(s) quoted. We do not expect systematic uncertainties to dominate and therefore do not consider them.

tometry are lower (because of the restriction to 1–300 GeV photons and because not all  $>1$  GeV photons fall within our aperture) and the background is higher (because the simple aperture cut allows more photons from other sources) but the average flux before the disappearance was  $2.22(14) \times 10^{-9} \text{ cm}^{-2} \text{ s}^{-1}$ , while the post-disappearance average flux is  $6.9(9) \times 10^{-9} \text{ cm}^{-2} \text{ s}^{-1}$ .

To better determine when the  $\gamma$ -ray flux started increasing, we used our aperture-photometry data and combined 2.5-Ms chunks starting every 500 ks. The results are plotted in the lower panel of Figure 1. This procedure unavoidably smoothes all features by 2.5 Ms (about 1 month). Nonetheless, it is clear that the  $\gamma$ -ray flux began rising at approximately the same time that the radio pulsations disappeared. It is unclear, however, whether the flux rose abruptly and then remained constant or whether it rose gradually and is possibly continuing to rise.

To look for spectral changes in a nearly model-independent way, we computed “hardness ratios” before and after the radio disappearance. Examination of the aperture photometry photons revealed that about half of them were above 1.6 GeV, so we simply performed aperture photometry as described above but with separate energy ranges of 1–1.6 GeV and 1.6–300 GeV. A “hardness ratio” would then be a ratio of (exposure-corrected) count rates in these two energy ranges. The hardness ratio before the radio disappearance was 1.10(12), while after the disappearance it was 1.4(3). We do not claim any significant change in hardness. Because of the low number of photons, we were not very sensitive to spectral changes.

We investigated orbital modulation of the  $\gamma$ -ray emission by using `tempo2` (Hobbs et al. 2006) with the `fermi` plugin to assign the corresponding orbital phase to each probability-tagged photon. We used the weighted H test (Kerr 2011) to look for periodic modulation, obtaining a false positive probability of 0.66 — that is, for purely random phases there is a 66% probability of having greater deviation from uniformity than we detect. Testing with a simulated signal in which all source photons are distributed according to a sine wave produced a median false positive probability of 0.08. In other words, even with this very strong modulation, we would have had only a 50% chance of obtaining a detection better than  $1.4\sigma$ . So although we have tested for orbital modulation, our non-detection rules out only very sharply peaked orbital modulation. We investigated modulation at the pulsar period using `tempo2` to assign a pulse phase to each photon, then testing for periodicity as above. The false positive probability we obtained was 0.997. This method has the same lack of sensitivity as our search for orbital pulsations, but it also has another limitation: because our orbital ephemeris for J1023 was last updated before its disappearance in radio, and because J1023 undergoes apparently random orbital period variations (Archibald et al. 2010, 2013), we should expect phase prediction errors as large as  $\sim 0.2$  turns to smear out any high harmonic content. It is therefore difficult to rule out even very-sharp-peaked pulsations.

### 3.3. X-ray results

The *Swift*/BAT finds only non-detections throughout the monitoring, with all measurement points having a significance  $< 3\sigma$ . We simulated X-ray spectra with a power law of spectral index between  $\Gamma = 1$  and  $\Gamma = 2$  and normalization set by using the *Swift*/XRT 0.5–10-keV luminosity reported in Patruno et al. (2013). For a spectral index  $\Gamma \geq 1.3$  we infer a 15–50 keV source luminosity below  $2 \times 10^{35} \text{ erg s}^{-1}$ , which is compatible with the *Swift*/BAT non-detections and the currently measured spectral index of the source ( $\Gamma \simeq 1.7$ ).

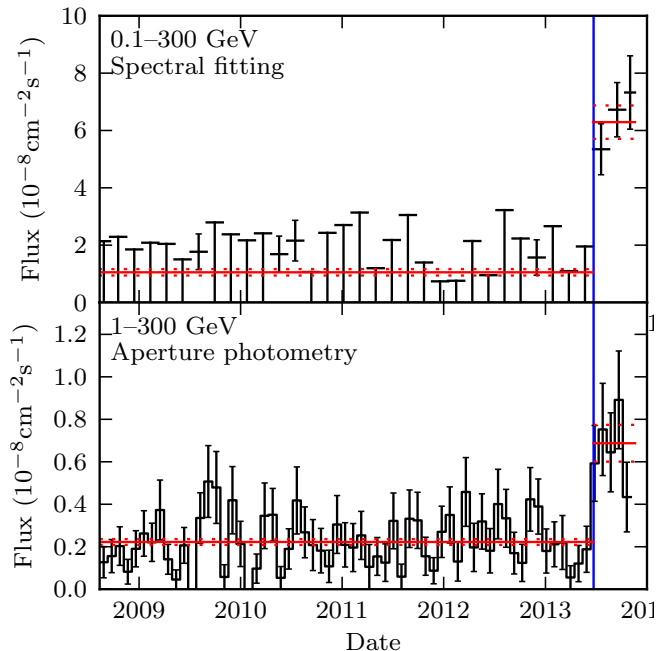


**Figure 2.**  $\gamma$ -ray photon flux from J1023. Top panel: The 100 MeV–300 GeV flux determined by spectral fitting, with uncertainties reported by the *Fermi* tool `gtlike`. For time bins in which the Test Statistic ( $\sim \sigma^2$ ) is less than 9 we instead computed and plotted 95% upper limits. The blue line marks 2013 June 30, the approximate date of the disappearance. The red lines show flux computed using all the before-disappearance data and all the after-disappearance data, and the dotted lines show the reported uncertainties on their values. Bottom panel: The 1–300 GeV flux determined by aperture photometry, with Poisson uncertainties. The blue line marks the first radio non-detection as above. The red lines show the average flux before and after 2013 June 30, and the dotted lines show the (Poisson) uncertainties on their values.

## 4. DISCUSSION

We report that, some time between 2013 June 15 and June 30, pulsations from the millisecond pulsar in the J1023 binary system disappeared at radio frequencies where they are otherwise easily detectable. Concurrent with this disappearance we find that the  $\gamma$ -ray flux of J1023 has increased five-fold. Subsequent optical, UV and X-ray observations have shown that an accretion disk has formed in the binary system (Halpern et al. 2013; Patruno et al. 2013), signifying that J1023 has undergone a transition from a binary MSP to an LMXB. The present transition appears similar to that of 2000/2001; the archival study by Archibald et al. (2009) shows the system transitioning from a radio point source and G-type optical colors to having an accretion disk.

We are now fortunate to observe two redback systems that have transitioned multiple times between LXMB and MSP states. Although its 2013 outburst is a uniquely observed event for a known MSP, as a radio pulsar M28I is fairly typical in a population of about 11 known GC redbacks<sup>17</sup>. This suggests that other similar pulsars in the Galactic GC system will also undergo such events in the coming years and decades. These sources remain challenging to study at optical and radio wavelengths, however, because of the relatively large distance to the most massive GCs ( $\sim 5-10$  kpc). Furthermore, since exchange interactions are common in GCs, some GC redbacks host neutron stars that are likely *not* orbited by their original binary companions. Although they are undoubtedly interesting test beds for studying the accretion process, it is less clear whether they are useful for understanding the long-term evolution from LMXBs to MSPs in the field. In contrast, the known field redbacks, of which J1023 was the first discovered, are typically significantly less distant ( $< 2$  kpc) and offer better potential for detailed multi-wavelength study. There are now at least 7 redbacks and 17 black widow systems known in the field, thanks in large part to targeted searches of unassociated *Fermi* sources (Ray et al. 2012). Again, as a radio pulsar, J1023 is no longer very atypical, with several similar examples, such as PSR J2215+5135 (Hessels et al. 2011), which has nearly identical orbital parameters and a likely similar, Roche-lobe-filling companion (Breton et al. 2013). Here as well, given proper radio, optical, and X-ray monitoring, it is expected that it may not be long before these similar systems show transitions like those we have observed from J1023. If, not, then the distinction of J1023 needs to be considered more carefully.

Though J1023 and M28I show many striking similarities in their X-ray behavior (Patruno et al. 2013), the former has yet to enter a truly energetic outburst state in which the accretion flow is reaching the neutron star surface. Indeed, the 2013 June to October activity of J1023 is arguably very similar to its past 2001 state (though no targeted X-ray data was available at that time). An energetic outburst like that seen in M28I (Papitto et al. 2013) can be ruled out for J1023 since 1996 because it would have triggered an all-sky X-ray monitor. M28I has also been observed for  $\sim 200$  ks by *Chandra* in 2008 (Linares et al. 2013), switching several times between a bright “active” ( $4 \times 10^{33}$  erg s<sup>-1</sup>) and a faint “passive” state ( $6 \times 10^{32}$  erg s<sup>-1</sup>). Therefore M28I can undergo rapid X-ray flux variations similar to those currently seen in J1023<sup>18</sup>. If the X-ray flux variations observed in M28I in quiescence (i.e., the 2008 *Chandra* data, for which no simultaneous radio observation is available) can be ascribed to the presence of an accretion disk, then there is no specific reason to presume that these two systems are

fundamentally different.

Shvartsman (1970) proposed that an active radio pulsar in a contact binary is able to prevent the formation of an accretion disk. However, M28I has shown beyond any doubt a luminous X-ray outburst in 2013 April. In all likelihood J1023 is also capable of undergoing a full accretion episode, although the recurrence time could be on the order of decades. Burderi et al. (2001) proposed that an LMXB can turn into a radio pulsar either cyclically or indefinitely depending on the orbital period of the system. According to Burderi’s definition, J1023 falls among the sources that cyclically alternate between an outburst and a radio pulsar state. Ekşİ & Alpar (2005) showed that an active pulsar does not necessarily imply the complete destruction of the accretion disk if the inner disk is truncated at 2–3 light cylinder radii. It is possible therefore that J1023 is an active pulsar surrounded by an accretion disk truncated outside the light cylinder. We suggest that both J1023 and M28I can probably exhibit three states characterized by i) an observable radio MSP and a low X-ray luminosity which is rotation powered ii) the presence of an accretion disk in a quiescent-like LMXB system, and iii) an AMXP, with high X-ray luminosity, powered by accretion, and potentially Type I X-ray bursts.

Regardless of the fact that the radio pulsar is currently not detectable, it appears most likely that J1023’s rotation-powered pulsar mechanism, most importantly the relativistic particle wind that is created, is still active. Before its recent state change, the  $\gamma$ -rays from the system were quite likely of magnetospheric origin, in analogy with other similar MSPs detected by *Fermi* LAT. As suggested by Tam et al. (2010), a portion of the  $\gamma$ -rays could be from an intra-binary shock between the pulsar and its companion star. However, for the  $\gamma$ -ray data preceding 2013 June, Archibald et al. (2013) show that, while there is a marginally significant detection of pulsations from J1023, there is no evidence for orbital modulation.

Searches for orbital-phase-dependent  $\gamma$ -ray variability in other similar systems have also been unsuccessful, again arguing that the observed emission from MSPs is predominantly magnetospheric when the source is in the radio-loud state. Other similar  $\gamma$ -ray MSPs are stable in flux, as are (almost) all young pulsars detected in  $\gamma$ -rays (Abdo et al. 2013). Recently the identification of  $\gamma$ -ray flux variability from PSR J2021+4026 (Allafort et al. 2013) showed that some  $\gamma$ -ray pulsars can undergo mode switches, reminiscent of recent discoveries in the radio (Kramer et al. 2006; Lyne et al. 2010). More recently, Hermsen et al. (2013) showed that for PSR B0943+10 there is a correlated mode switch in both radio and X-rays, providing strong evidence that a sudden and global magnetospheric state change can occur. However, while mode switching is a well known phenomenon observed in several slowly rotating radio pulsars, there is as yet no evidence that such magnetospheric switching occurs in MSPs. Therefore, the five-fold increase of the  $\gamma$ -ray flux in the current state is unlikely to be of magnetospheric origin or precipitated by a change associated with the pulsar itself.

In light of this, it appears more likely that the source of the increased  $\gamma$ -ray flux must be an increased shock

<sup>17</sup> <http://www.naic.edu/~pfreire/GCpsr.html>

<sup>18</sup> Papitto et al. (2013) describes the 2008 *Chandra* active and passive states as an “outburst” followed by a “total quenching” of the X-ray luminosity. We clarify, however, that the active/passive states cannot be considered as a standard outburst/quiescent cycle. The active state is indeed too faint and within the range of quiescent luminosities of LMXBs. Furthermore the passive state displays a significant X-ray luminosity well above the background level and therefore cannot be truly defined as quenching (see Linares et al. (2013) for an extended discussion).

within the system. The striking correlation with the timing of the radio shut-off indicates that this rise in  $\gamma$ -rays must be closely related to the reappearance of an accretion disk in the system (Patruno et al. 2013), which is likely the principal driving force behind the observed changes in the radio, optical, X-ray, and  $\gamma$ -ray emission. We suggest that to produce the excess  $\gamma$ -rays requires both an active pulsar wind and an accretion disk, but that there can be no active accretion onto the neutron star, which would quench the pulsar mechanism and hence the relativistic wind.

If the rotation-powered pulsar is still active, enshrouding of the system by intra-binary material, causing severe scattering and/or absorption, is the logical explanation for the absence of radio pulsations. This would make J1023 a so-called “hidden” radio MSP, as hypothesized by Tavani (1991). In this scenario, the MSP is completely enshrouded in the prodigious outflow from its close companion star, rendering the pulsar perpetually eclipsed at radio frequencies. At the same time, the system generates strong un-pulsed shock emission in X-rays and  $\gamma$ -rays, due to the interaction of the pulsar wind with the outflow of matter (Tavani 1993). Other recently discovered eclipsing MSPs also exhibit compelling evidence for enshrouding (Romani & Shaw 2011; Ray et al. 2013), though J1023 is the first instance where we see a sudden increase in the high-energy emission, correlated with a radio disappearance. Together, these systems support previous arguments that a non-negligible fraction of MSPs may often be non-detectable at radio wavelengths because of enshrouding. There is also some evidence that this becomes more problematic for the fastest-spinning MSPs (Hessels et al. 2006, 2008)<sup>19</sup>.

Spin-down luminosity is a sensitive function of spin period ( $\dot{E} \propto \dot{P}/P^3$ ) and hence this may explain this trend, all other factors, like orbital separation and companion type, being equal. Indeed this could be one reason for the absence of a discovery of a sub-millisecond pulsar thus far, in spite of reasonable sensitivity to such sources in modern large-scale pulsar surveys, such as the PALFA survey (Cordes et al. 2006) and the HTRU survey (Keith et al. 2010) and the aforementioned LAT-directed searches. On the other hand, the existence of many such “hidden” fast radio MSPs is problematic in light of the absence of detections of accreting MSPs with frequency higher than 619 Hz, in spite of there being no obvious selection effects against finding them with X-ray telescopes (Chakrabarty et al. 2003). J1023 is a 1.7-ms pulsar, the fifth fastest spinner known in the Galactic field. Of the five fastest-spinning MSPs in the field, three are known to eclipse and the other two are isolated.

With the re-appearance of an accretion disk, J1023 also resembles a number of LMXB systems containing AMXPs. It has been suggested that some AMXPs reactivate as rotation-powered pulsars in quiescence (Campana et al. 1998, 2004). Apart from M28I, no radio pulsations have been detected from any AMXP in quiescence, although this could be a consequence of enshrouding as

well. In addition, none has yet been detected as  $\gamma$ -ray sources with *Fermi* LAT (Xing & Wang 2013), although they are all significantly more distant than J1023. It is thus plausible that quiescent AMXPs may also be “hidden” MSPs.

Given the nature of the enhanced  $\gamma$ -ray emission that has appeared from J1023, one may consider what similarities exist with the small population of  $\gamma$ -ray binaries, where a compact object is orbited by a massive OB star (e.g. Dubus 2013). Still the best understood high-mass gamma-ray binary is PSR B1259–63, which contains a relatively rapidly-rotating (P=47 ms) young radio pulsar; its pulsar has  $\dot{E} \sim 20$  times higher than that of PSR J1023+0038 yet has shown  $\gamma$ -rays  $\sim 200$  times brighter, achieving near 100% efficiency in converting spin-down power to  $\gamma$ -rays near periastron, when the pulsar’s wind is shocked closest to the pulsar. Though the orbital compactness and companion mass in the case of J1023 is quite different when compared with such systems, there may be similarities in some of the physical mechanisms at play. This suggests PSR J1023+0038 could indeed continue to brighten. It may also serve a similar prototype role for a new class of low-mass  $\gamma$ -ray binaries. We note that given its increased  $\gamma$ -ray luminosity, its present  $\gamma$ -ray efficiency, assuming an isotropic luminosity and taking  $\dot{E} = 4.3 \times 10^{34}$  erg/s (Deller et al. 2012), is 0.14. We therefore expect that the  $\gamma$ -ray luminosity will rise at most another factor of 7, as beyond that it would exceed the available energy from pulsar spin-down.

Regardless of J1023’s upcoming X-ray behavior, when it returns to an MSP state then it will be possible to compare the radio pulsar timing before and after the current active state. J1023 benefits greatly in this regard from its relative brightness and the high cadence of our recent radio monitoring observations. It also does not suffer from the contaminating influence of acceleration in a GC gravitational potential, as in the case of M28I. After being spun-up to millisecond periods, an accreting neutron star should enter a spin-down phase where the mass transfer rate decreases due to the progressive detachment of the donor radius from its Roche lobe. During this final evolutionary phase the neutron star magnetosphere expands substantially and a large fraction of the neutron star rotational energy is lost via a propeller-like mechanism (Tauris 2012). It is possible therefore that what we are observing in J1023 is indeed this very last phase of its life as an LMXB. In this case it should be possible to observe a strong spin down during this active phase i.e. well in excess of the pulsar magnetic dipole spin down. Even if no accretion-powered X-ray pulsations are detected, this test can be performed once the active phase is over by comparing the pre- and post-active phase radio timing solutions.

In conclusion, we have demonstrated a new stage in the back-and-forth transitioning that seems to characterize the reback class of MSPs. For the first time, we have seen a bright radio MSP become undetectable while at the same time the system becomes  $\gamma$ -ray bright. We argue that the pulsar mechanism remains active in this system, but that the radio pulsations are obscured. While higher-frequency radio observations have also been unsuccessful, there is perhaps potential for detecting pulsed X-rays (not generated by accretion) that will further con-

<sup>19</sup> Nonetheless, despite observational biases against finding fast-spinning MSPs as well as a possible population of fast-spinning, “hidden” MSPs, the spin frequency distribution of MSPs is clearly seen to drop off rapidly toward higher frequencies (Hessels et al. 2007, see his Fig 4.)

firm the continued activity of the pulsar itself. The detection or lack of accretion-powered X-ray pulsations in forthcoming X-ray observations can easily disprove or strengthen such an hypothesis. Similarly, planned radio interferometric observations to look for a continuum radio source are also important in this regard.

The analogy with the wider-orbit, much more massive companion  $\gamma$ -ray binaries is tantalizing. A multi-wavelength campaign that follows J1023 back into its radio MSP state may better resolve the state transition and associated radio/optical/X-ray/ $\gamma$ -ray phenomenology. Long-term, phase-coherent timing will also shed light on the accretion torques experienced while the radio pulsar was undetectable.

We thank H.A. Krimm for kind support in the use of the *Swift*/BAT data. A.P. acknowledges support from the Netherlands Organization for Scientific Research (NWO) Vidi fellowship. A.M.A. and J.W.T.H. acknowledge funding for this work from an NWO Vrije Competitie grant. The WSRT is operated by ASTRON with support from NWO. Pulsar observations with the Lovell Telescope are funded through a consolidated grant from STFC. The Fermi LAT is a pair conversion telescope designed to cover the energy band from 20 MeV to greater than 300 GeV. It is the product of an international collaboration between NASA and DOE in the U.S. and many scientific institutions across France, Italy, Japan and Sweden. The GBT is operated by the National Radio Astronomy Observatory (NRAO). NRAO is a facility of the NSF operated under cooperative agreement by Associated Universities, Inc. The Arecibo Observatory is operated by SRI International under a cooperative agreement with the NSF (AST-1100968), and in alliance with Ana G. Méndez-Universidad Metropolitana, and the Universities Space Research Association. The *Fermi* LAT Collaboration acknowledges support from a number of agencies and institutes for both development and the operation of the LAT as well as scientific data analysis. These include NASA and DOE in the United States, CEA/Irfu and IN2P3/CNRS in France, ASI and INFN in Italy, MEXT, KEK, and JAXA in Japan, and the K. A. Wallenberg Foundation, the Swedish Research Council and the National Space Board in Sweden. Additional support from INAF in Italy and CNES in France for science analysis during the operations phase is also gratefully acknowledged. ABH acknowledges that this research was supported by a Marie Curie International Outgoing Fellowship within the 7th European Community Framework Programme (FP7/2007–2013) under grant agreement no. 275861.

#### REFERENCES

- Abdo, A. A., Ajello, M., Allafort, A., et al. 2013, *ApJS*, 208, 17  
 Ackermann, M., Ajello, M., Albert, A., et al. 2012, *ApJS*, 203, 4  
 Allafort, A., Baldini, L., Ballet, J., et al. 2013, *ApJ*, 777, L2  
 Alpar, M. A., Cheng, A. F., Ruderman, M. A., & Shaham, J. 1982, *Nature*, 300, 728  
 Archibald, A. M., Kaspi, V. M., Bogdanov, S., et al. 2010, *ApJ*, 722, 88  
 Archibald, A. M., Kaspi, V. M., Hessels, J. W. T., et al. 2013, arXiv:1311.5161, submitted  
 Archibald, A. M., Stairs, I. H., Ransom, S. M., et al. 2009, *Science*, 324, 1411  
 Atwood, W. B., Abdo, A. A., Ackermann, M., et al. 2009, *ApJ*, 697, 1071  
 Backer, D. C., Kulkarni, S. R., Heiles, C., Davis, M. M., & Goss, W. M. 1982, *Nature*, 300, 615  
 Bailes, M., Bates, S. D., Bhalariao, V., et al. 2011, *Science*, 333, 1717  
 Bogdanov, S., Archibald, A. M., Hessels, J. W. T., et al. 2011, *ApJ*, 742, 97  
 Bond, H. E., White, R. L., Becker, R. H., & O'Brien, M. S. 2002, *PASP*, 114, 1359  
 Breton, R. P., van Kerkwijk, M. H., Roberts, M. S. E., et al. 2013, *ApJ*, 769, 108  
 Burderi, L., Possenti, A., D'Antona, F., et al. 2001, *ApJ*, 560, L71  
 Campana, S., Stella, L., Mereghetti, S., et al. 1998, *ApJ*, 499, L65+  
 Campana, S., D'Avanzo, P., Casares, J., et al. 2004, *ApJ*, 614, L49  
 Chakrabarty, D., Morgan, E. H., Munro, M. P., et al. 2003, *Nature*, 424, 42  
 Cordes, J. M., Freire, P. C. C., Lorimer, D. R., et al. 2006, *ApJ*, 637, 446  
 Deller, A. T., Archibald, A. M., Brisken, W. F., et al. 2012, *ApJ*, 756, L25  
 Dubus, G. 2013, *A&A Rev.*, 21, 64  
 Ekşil, K. Y., & Alpar, M. A. 2005, *ApJ*, 620, 390  
 Fruchter, A. S., Berman, G., Bower, G., et al. 1990, *ApJ*, 351, 642  
 Halpern, J. P., Gaidos, E., A., S., & Price-Whelan, A. M. and Bogdanov, S. 2013, *The Astronomer's Telegram*, 5514, 1  
 Hermsen, W., Hessels, J. W. T., Kuiper, L., et al. 2013, *Science*, 339, 436  
 Hessels, J. W. T., Ransom, S. M., Kaspi, V. M., et al. 2008, in *American Institute of Physics Conference Series*, Vol. 983, 40  
 Years of Pulsars: Millisecond Pulsars, Magnetars and More, ed. C. Bassa, Z. Wang, A. Cumming, & V. M. Kaspi, 613–615  
 Hessels, J. W. T., Ransom, S. M., Stairs, I. H., et al. 2006, *Science*, 311, 1901  
 Hessels, J. W. T., Ransom, S. M., Stairs, I. H., Kaspi, V. M., & Freire, P. C. C. 2007, *ApJ*, 670, 363  
 Hessels, J. W. T., Roberts, M. S. E., McLaughlin, M. A., et al. 2011, in *American Institute of Physics Conference Series*, Vol. 1357, *American Institute of Physics Conference Series*, ed. M. Burgay, N. D'Amico, P. Esposito, A. Pellizzoni, & A. Possenti, 40–43  
 Hobbs, G. B., Edwards, R. T., & Manchester, R. N. 2006, *MNRAS*, 369, 655  
 Homer, L., Szkody, P., Chen, B., et al. 2006, *AJ*, 131, 562  
 Karuppusamy, R., Stappers, B., & van Straten, W. 2008, *PASP*, 120, 191  
 Keith, M. J., Jameson, A., van Straten, W., et al. 2010, *MNRAS*, 407, 1356  
 Kerr, M. 2011, *ApJ*, 732, 38  
 Kramer, M., Lyne, A. G., O'Brien, J. T., Jordan, C. A., & Lorimer, D. R. 2006, *Science*, 312, 549  
 Krimm, H. A., Holland, S. T., Corbet, R. H. D., et al. 2013, *ApJS*, 209, 14  
 Linares, M., Bahramian, A., Heinke, C., et al. 2013, *ArXiv e-prints*, arXiv:1310.7937  
 Lyne, A., Hobbs, G., Kramer, M., Stairs, I., & Stappers, B. 2010, *Science*, 329, 408  
 Nolan, P. L., Abdo, A. A., Ackermann, M., et al. 2012, *ApJS*, 199, 31  
 Papitto, A., Ferrigno, C., Bozzo, E., et al. 2013, *Nature*, 501, 517  
 Patruno, A., & Watts, A. L. 2012, *ArXiv e-prints*, arXiv:1206.2727  
 Patruno, A., Archibald, A. M., Hessels, J. W. T., et al. 2013, *ArXiv e-prints*, arXiv:1310.7549  
 Radhakrishnan, V., & Srinivasan, G. 1981, in *Proc. 2nd Asian-Pacific Regional Meeting of the IAU*, ed. B. Hidayat & M. W. Feast (Jakarta: Tira Pustaka), 423–432  
 Ransom, S. M. 2013, in *IAU Symposium*, Vol. 291, *IAU Symposium*, 3–10  
 Ray, P. S., Abdo, A. A., Parent, D., et al. 2012, *ArXiv e-prints*, arXiv:1205.3089  
 Ray, P. S., Ransom, S. M., Cheung, C. C., et al. 2013, *ApJ*, 763, L13

- Roberts, M. S. E. 2011, in American Institute of Physics Conference Series, Vol. 1357, American Institute of Physics Conference Series, ed. M. Burgay, N. D'Amico, P. Esposito, A. Pellizzoni, & A. Possenti, 127–130
- Romani, R. W., & Shaw, M. S. 2011, ApJ, 743, L26
- Ryba, M. F., & Taylor, J. H. 1991, ApJ, 380, 557
- Shvartsman, V. F. 1970, Soviet Ast., 14, 527
- Stappers, B. W., Bailes, M., Lyne, A. G., et al. 1996, ApJ, 465, L119
- Tam, P. H. T., Hui, C. Y., Huang, R. H. H., et al. 2010, ApJ, 724, L207
- Tauris, T. M. 2012, Science, 335, 561
- Tavani, M. 1991, Nature, 351, 39
- . 1993, ApJ, 407, 135
- Thorstensen, J. R., & Armstrong, E. 2005, AJ, 130, 759
- van Haften, L. M., Nelemans, G., Voss, R., & Jonker, P. G. 2012, A&A, 541, A22
- van Straten, W., & Bailes, M. 2011, PASA, 28, 1
- van Straten, W., Demorest, P., & Osłowski, S. 2012, Astronomical Research and Technology, 9, 237
- Wijnands, R., & van der Klis, M. 1998, Nature, 394, 344
- Woudt, P. A., Warner, B., & Pretorius, M. L. 2004, MNRAS, 351, 1015
- Xing, Y., & Wang, Z. 2013, ApJ, 769, 119